Surv Geophys (2015) 36:851–859
DOI 10.1007/s10712-015-9342-2

A Statistical Study of Lightning Activities and $M \geq 5.0$ Earthquakes in Taiwan During 1993–2004

J. Y. Liu[1,2] · Y. I. Chen[3] · C. H. Huang[1,3] · Y. Y. Ho[4] · C. H. Chen[5]

Received: 1 December 2014 / Accepted: 21 September 2015 / Published online: 13 October 2015

Abstract In this study, to see whether or not lightning activities are related to earthquakes, we statistically examine lightning activities 30 days before and after 78 land and 230 sea $M \geq 5.0$ earthquakes in Taiwan during the 12-year period of 1993–2004. Lightning activities versus the location, depth, and magnitude of earthquakes are investigated. Results show that lightning activities tend to appear around the forthcoming epicenter and are significantly enhanced a few, especially 17–19, days before the $M \geq 6.0$ shallow (depth $D \leq 20$ km) land earthquakes. Moreover, the size of the area around the epicenter with the statistical significance of lightning activity enhancement is proportional to the earthquake magnitude.

Keywords Binomial test · Earthquake · Lightning activities

1 Introduction

Seismo-electromagnetic anomalies (SEAs) of electromagnetic waves, electric fields, magnetic fields, etc. in the lithosphere, atmosphere, and ionosphere prior to large earthquakes have been intensively investigated (e.g., Hayakawa and Fujinawa 1994; Hayakawa 1999; Hayakawa and Molchanov 2002; Pulinets and Boyarchuk 2004). One of the most

✉ J. Y. Liu
tigerjyliu@gmail.com

1 Institute of Space Science, National Central University, Chung-Li 320, Taiwan

2 Center for Remote Sensing, National Central University, Chung-Li 320, Taiwan

3 Institute of Statistics, National Central University, Chung-Li 320, Taiwan

4 Institute of Earth Sciences, Academia Sinica, Taipei 115, Taiwan

5 Department of Earth and Environmental Sciences, National Chung Cheng University, Chiayi 621, Taiwan

convincing signatures caused by SEAs is anomalous values of the GPS total electron content (TEC) in the ionosphere appearing before devastating large earthquakes, such as 1999 *M*7.6 Chi-Chi, 2004 *M*9.3 Sumatra, 2008 *M*7.9 Wenchuan, and 2010 *M*7.0 Haiti earthquake (Liu et al. 2001, 2009, 2010, 2011). Several models of the lithosphere–atmosphere–ionosphere coupling via the global electric circuit have been proposed to develop a physical understanding of the reported SEAs (Harrison et al. 2010, 2014; Kim et al. 2012; Kuo et al. 2011; Pulinets and Davidenko 2014).

On the other hand, earthquake lights and luminous phenomena are spectacular features and have been often observed (Derr 1973, 1986; Heraud and Lira 2011). Scientists propose that the crust deformation activates and releases gases/electrical charges, which then generate the atmospheric electric field and currents, and in turn affect the atmospheric electric circuit possibly resulting in luminous phenomena before and during large earthquakes (Lockner et al. 1983; Finkelstein and Powell 1970; Freund 2000; Harrison et al. 2010, 2014; Kim et al. 2012; Kuo et al. 2011; Pulinets and Boyarchuk 2004; St-Laurent et al. 2006). Enomoto and Zheng (1998) observe the roots of plants being charred near the epicenter of the 17 January 1995 *M*6.9 Kobe earthquake. They suggest that electric currents from earthquake lightning passed through the charred roots. Recently, Kuo et al. (2011, 2014) extend their upper atmospheric lightning model by injecting the atmospheric electric currents and/or electric fields generated during the earthquake period to explain

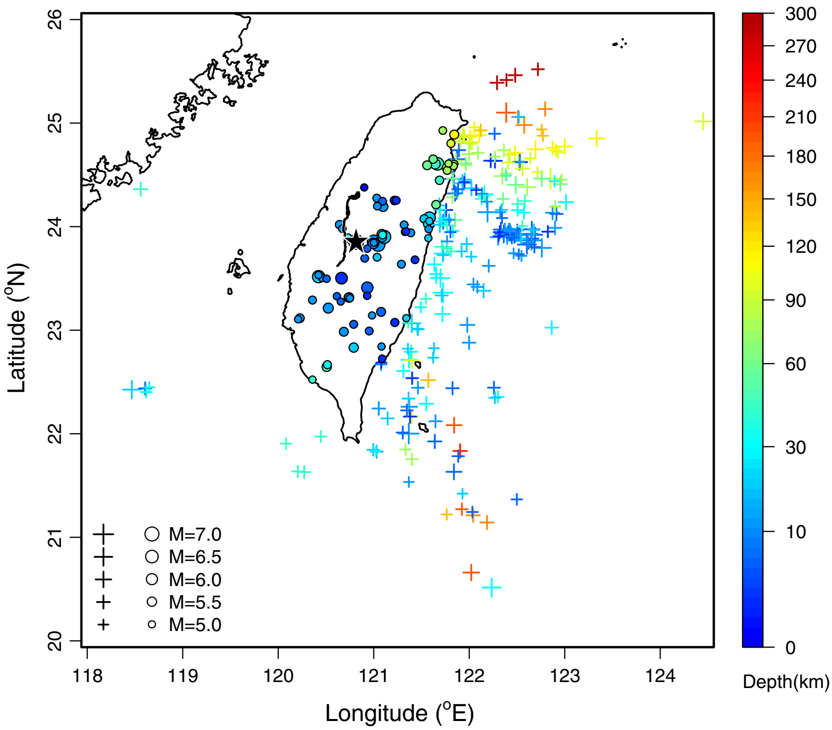

Fig. 1 The locations of the 308 $M_L \geq 5.0$ earthquakes that occurred in the Taiwan region during 1993–2004. The *circle and cross symbols* denote the 78 land and 230 sea earthquakes, respectively. The *black star and curve* denote the 21 September 1999 M7.6 Chi-Chi earthquake (23.86N, 120.82E) and the Chelungpu fault, respectively

ionospheric TEC anomalies before large earthquakes. Thus, the lightning activity is one of the key parameters to understand the atmospheric electric fields near the Earth's surface (Rakov and Uman 2003) and the lithosphere–atmosphere–ionosphere coupling during the earthquake preparation period (Pulinets and Boyarchuk 2004; Pulinets and Davidenko 2014). In this paper, we statistically survey and report the relationship between lightning occurrence and 395 $M \geq 5.0$ earthquakes in Taiwan during 1993–2004.

2 Observation

On average, a $M \geq 5.0$ earthquake occurs in Taiwan every 10–14 days (Liu et al. 2006). Figure 1 reveals that 395 $M \geq 5.0$ earthquakes occurred in Taiwan from 1993 to 2004. Such a high earthquake recurrence rate provides us an excellent chance to investigate the lightning activities possibly associated with large earthquakes. Figure 2 shows that lightning occurrence along the Chelungpu fault was significantly enhanced on days 20–30 and 2–7 prior to the 21 September 1999 (0147LT) *M*7.6 Chi-Chi earthquake. To find whether such an enhancement is also likely to appear before other earthquakes, a statistical analysis is implemented to examine lightning occurrence associated with 395 $M \geq 5.0$ earthquakes, occurring over 308 earthquake days in Taiwan during the 12-year period of 1993–2004 (Fig. 1). When several $M \geq 5.0$ earthquakes occur on the same day, only the larger or

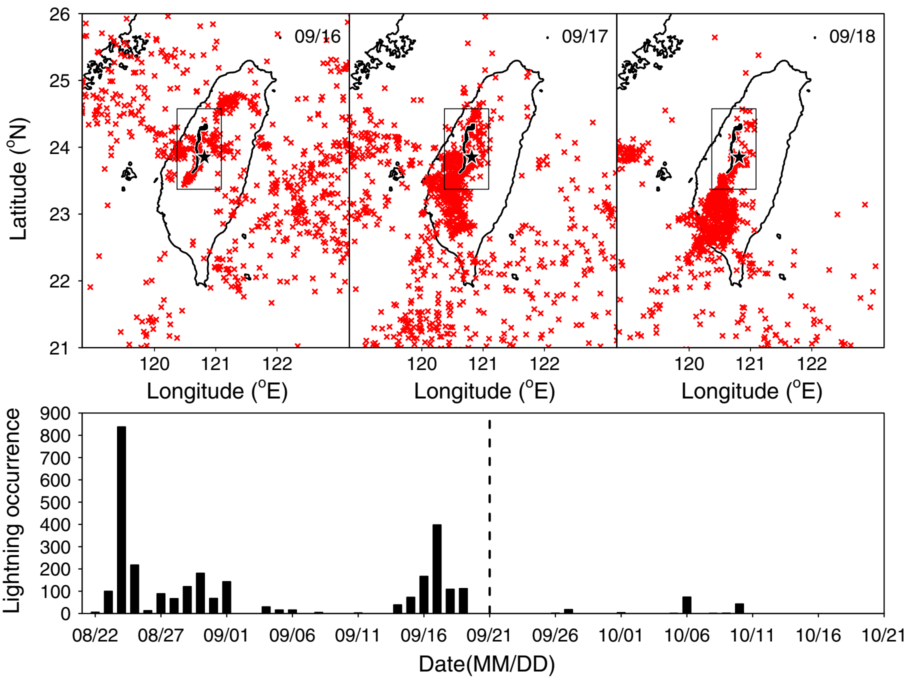

Fig. 2 Lightning activities during the 21 September 1999 *M*7.6 Chi-Chi earthquake. *Top panel* the spatial distribution of lightning on 16, 17 and 18 September are shown in the *upper panels*. *Lower panel* lightning occurrence/counts within 0.25° in latitude or longitude to the Chelungpu fault denoted by the rectangular box 1–30 days before and after the Chi-Chi earthquake. In fact, 90 % of the lightning occurred before the Chi-Chi earthquake in the 61 days of this study period

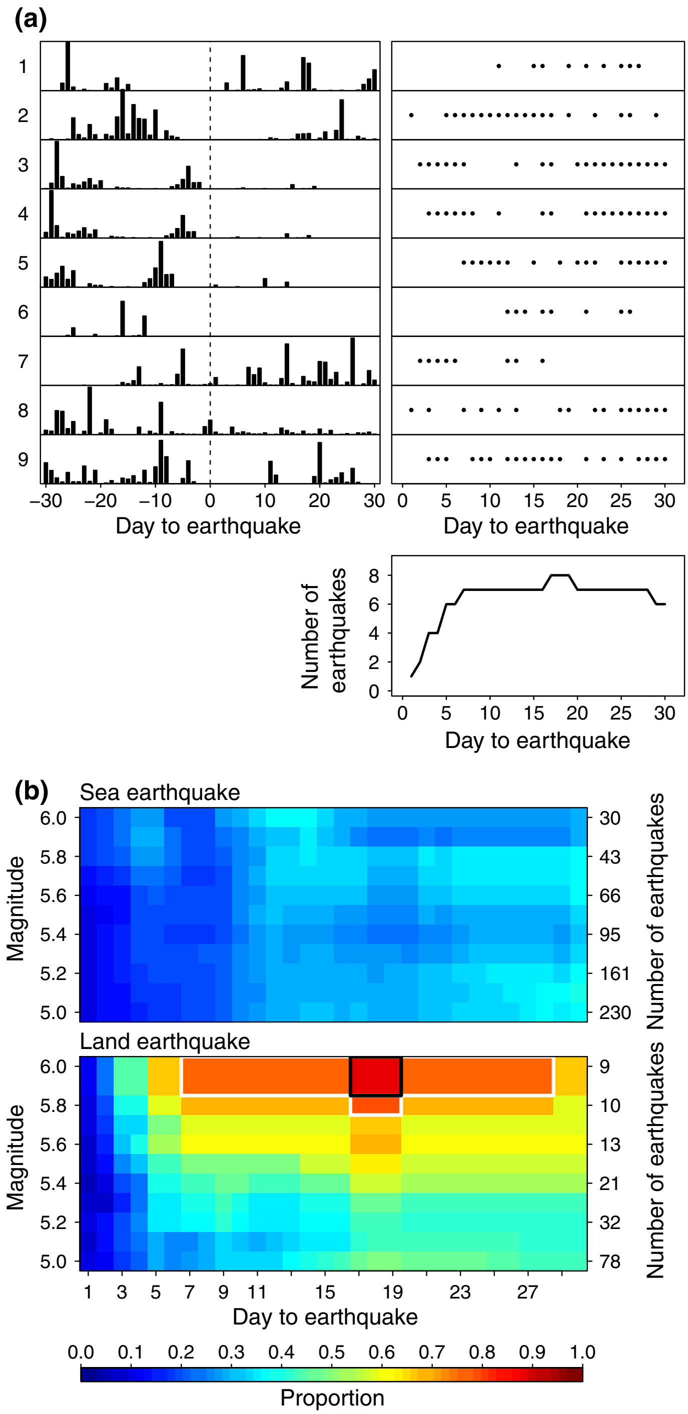
(a)
1
2
3
4
5
6
7
8
9
−30 −20 −10 0 10 20 30
Day to earthquake
0 5 10 15 20 25 30
Day to earthquake
Number of earthquakes
8 6 4 2 0
0 5 10 15 20 25 30
Day to earthquake
(b)
Sea earthquake
Magnitude
6.0 5.8 5.6 5.4 5.2 5.0
30 43 66 95 161 230
Number of earthquakes
Land earthquake
Magnitude
6.0 5.8 5.6 5.4 5.2 5.0
9 10 13 21 32 78
Number of earthquakes
1 3 5 7 9 11 15 19 23 27
Day to earthquake
0.0 0.1 0.2 0.3 0.4 0.5 0.6 0.7 0.8 0.9 1.0
Proportion

◀**Fig. 3** The proportions and associated *P* value of various earthquake magnitudes and cumulative days. **a** *Left panel* lightning activities during each $M \geq 6.0$ land earthquake; *right top panel* PELA (pre-earthquake lightning anomaly) within various cumulative days of each event; *lower right panel* reveals that the summation of the earthquake number with PELA for a certain cumulative day. **b** The proportions of the sea earthquakes (*upper*) and land earthquakes (*lower*) with PELA in various cumulative days and magnitudes. The earthquake numbers with different magnitudes are given at the *right-hand side*. The *black and white rectangular areas* denote *P* values being less than 0.05 and 0.10, respectively. The *P* value in the *black rectangle* is 0.02

largest one is denoted. Christian et al. (2003) globally study the annual frequency and distribution of lightning and confirm that lightning occurs mainly over land areas, with an average land/ocean ratio of about 10:1. Since lightning occurrence over the land is 4.63 times greater than that over the sea around Taiwan, we then examine lightning occurrence associated with the sea and land earthquakes separately.

3 Temporal Analysis

In total, there are 78 land and 230 sea $M \geq 5.0$ earthquake days. To minimize seasonal effects on the lightning activities, we examine the daily lightning frequencies within a 50 km × 50 km (North–South × East–West) area of the epicenter *d* cumulative days before and after the earthquakes with various magnitudes. When lightning occurrence within a certain cumulative day before the earthquake is more frequent than that after the earthquake, we refer to this as PELA (pre-earthquake lightning anomaly). We then count 1 for the cumulative day to the earthquake; otherwise, the count is 0. The proportion of the number of earthquakes with PELA to the total number of earthquakes under study is further computed. Figure 3a takes all 9 $M \geq 6.0$ land earthquakes during the observation period as an example. It can be seen that the proportion monotonically increases from day 1 to 7, becoming saturated thereafter, and yields maxima on days 17–19. Figure 3b illustrates the proportions of various magnitudes and cumulative days for both sea and land earthquakes. The proportions of sea earthquakes are less than 0.5, while those of land earthquakes increase with their magnitudes. It can be seen that a larger land earthquake yields a greater proportion within a shorter cumulative day, and more than 70 % of $M \geq 5.8$ land earthquakes are associated with the PELA for longer than seven cumulative days.

To further investigate whether the PELAs are significantly associated with those earthquakes, we consider the number of earthquakes (*X*) with PELA among the *n* earthquakes under study within *d* cumulative days to the earthquake. Note that *X* is distributed according to a binomial distribution with parameters *n* and *p*, the probability of observing PELA for the earthquake. When $p = 0.5$, the lightning activity is equally likely to occur before and after the earthquake. When $p > 0.5$, on the other hand, the lightning activity is more likely to occur before the earthquake than after. Therefore, we conduct a statistical test for $p = 0.5$ against $p > 0.5$. Suppose that the observed *X* is *x*. We then compute the associated *P* value as

$$P(X \geq x) = \sum_{y=x}^{n} p(y; n, 0.5),$$

where $p(y; n, 0.5) = \binom{n}{y}(0.5)^n$. Note that a small *P* value indicates that it is less likely to observe such a large value of *x* under $p = 0.5$. Therefore, under the significance level 0.05, we reject $p = 0.5$ and conclude $p > 0.5$, if the P value is smaller than 0.05. The P values, 0.05 and 0.10, of the test for a variety of the cumulative days and magnitudes of sea and land earthquakes are denoted in Fig. 3b. The large P values of about 1 show that there is no significant difference in lightning activities before and after sea earthquakes. By contrast, the P values are smaller than 0.1 for $M \geq 5.9$ during cumulative days 7–28. The P values smaller than 0.05 provide significant evidence for land earthquakes with PELA, which are corresponding to days 17–19 and magnitude greater than 5.9.

To understand the relationship between the occurrence of the PELAs and the parameters of the related earthquakes, the depths of the land earthquakes with/without PELAs on 18 cumulative days are plotted against the corresponding magnitudes (Fig. 4a). Results show that the $M \geq 6.0$ earthquakes with depth $D \leq 20$ km are more likely to experience PELA. To find the land earthquakes with certain depths (magnitudes) that are more likely to experience PELA, the odds of every 10 earthquakes (odds $= X/(n - X)$) sliding by 1 with

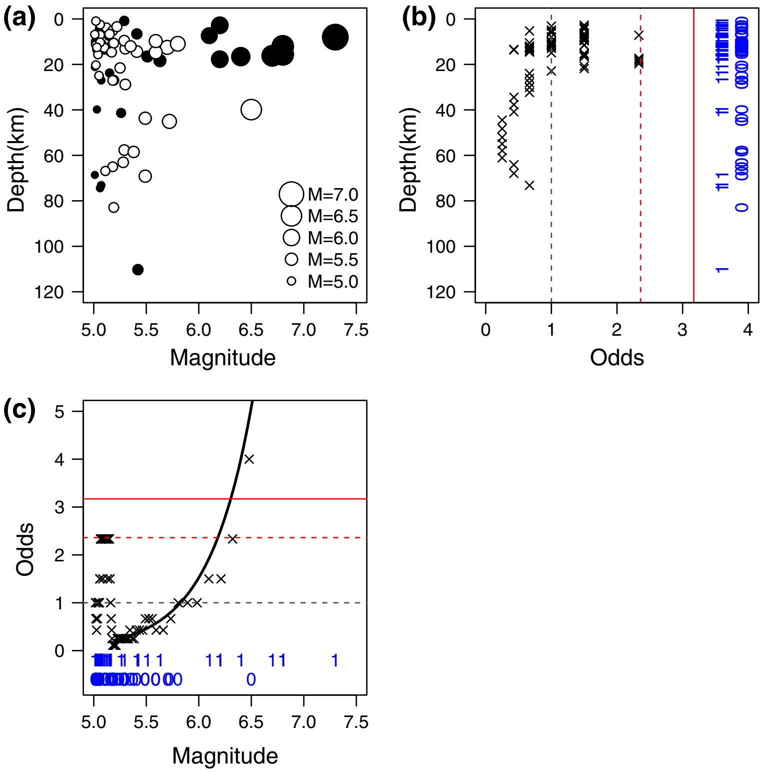

Fig. 4 The depth and magnitude of the earthquakes as well as the odds of PELA versus the depth and magnitude within 18 cumulative days. **a** The depths of the 78 land earthquakes versus the associated magnitudes. *Solid and empty circles* represent the earthquakes with and without the associated PELAs, respectively. **b** Odds (every 10 earthquakes sliding by 1 from shallow to deep depth) versus the related mean depth. **c** Odds (every 10 earthquakes sliding by 1 from small to large magnitude) versus the related mean magnitude. The fitted logistic regression (*black curve*) against the $M \geq 5.2$ earthquakes. One and zero represent the earthquakes with and without the associated PELAs, respectively. The *black dashed*, *red dashed*, and *red solid lines* denote the value of odds 1, 2.36 (significance level 0.1), and 3.17 (significance level 0.05), respectively

PELA are computed from small to large depths (magnitudes). Results show that the earthquakes with $M \geq 5.9$ or $D \leq 25$ km have a better chance of PELA occurrence (Fig. 4b, c). In fact, the $M \geq 5.9$ and $D \leq 25$ earthquakes all experience PELA (Fig. 4a). Moreover, on the basis of the 60 $M \geq 5.2$ land earthquake days, the fitted logistic regression model (Hosmer and Lemeshow 1989) for the logarithm of the odds of the earthquake with PELA to the earthquake magnitude is

$$\log\left(\frac{p}{1-p}\right) = 117.85 - 42.42M + 3.79M^2$$

The fitted curve presented in Fig. 4c indicates that the odds are increasing in magnitude, and $M \geq 6.4$ earthquakes have a significant chance to exhibit PELA. This finding demonstrates that PELA occurrence is proportional to the earthquake magnitude.

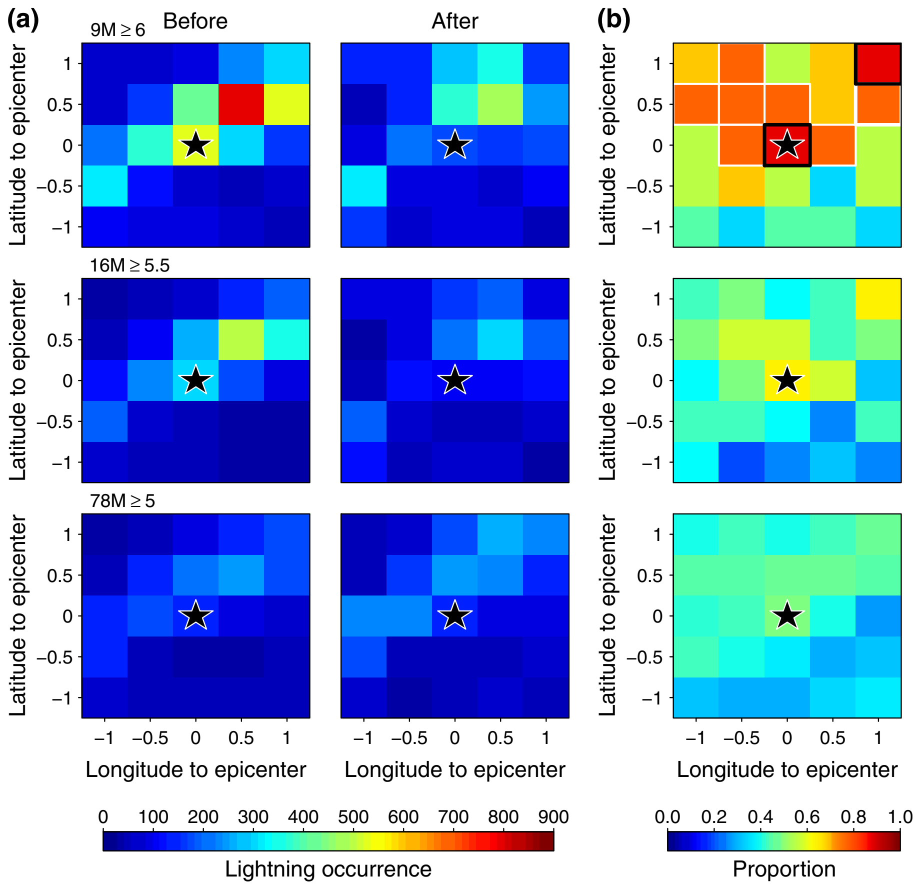

Fig. 5 Spatial distribution of lightning occurrence and the associated proportions with PELAs 18 cumulative days before and after the earthquakes. **a** Spatial distribution of lightning occurrence before (*left panel*) and after (*right panel*) $M \geq 5.0$, 5.5, and 6.0 earthquakes. **b** The proportions of PELAs for $M \geq 5.0$, 5.5, and 6.0 earthquakes. The *black and white square* areas denote P values being less than 0.05 and 0.10, respectively. The P value in the *black square* over the epicenter is 0.02

4 Spatial Analysis

To explore the lithosphere–atmosphere coupling, the spatial distributions of lightning near the epicenter within 18 cumulative days before and after the land earthquakes are investigated (Fig. 5a). When the earthquake magnitude is larger, the lightning activities become more frequent before the earthquake than after, as expected. The proportions in Fig. 5b reveal that the land earthquakes under study experience PELA most frequently near the epicenter. Moreover, for earthquakes with larger magnitudes, the prominent proportions expand over a larger area around the epicenter. The P values of 0.05 and 0.10 confirm that the PELAs around the epicenter of $M \geq 6.0$ land earthquake are statistically significant.

5 Discussion and Conclusion

Figure 3 reveals that a larger land earthquake yields a greater proportion P within a shorter cumulative day, while Fig. 5 shows that a larger earthquake has a larger significant area around the epicenter. Moreover, Fig. 4 shows that a larger and shallower earthquake has a better chance to experience lightning occurrence. These results suggest that a large shallow land earthquake inhabits a great energy and deformation area (Båth 1966; Lay and Wallace 1995; Dobrovolsky et al. 1979), which modifies the electromagnetic environment and in turn induces lightning occurrence during the earthquake preparation period. In conclusion, we have found statistically significant evidence that more lightning activity occurs around the epicenter a few days before larger shallow land earthquakes than at other times.

Acknowledgments Both the lightning data and earthquake catalog are obtained from Central Weather Bureau in Taiwan. This study has been partially supported by the project, MOST 103-2628-M-008-001, granted by Ministry of Science and Technology (MOST) to National Central University.

References

Båth M (1966) Earthquake energy and magnitude. Phys Chen Earth 7:115–165

Christian HJ et al (2003) Global frequency and distribution of lightning as observed from space by the optical transient detector. J Geophys Res 108(D1):4005. doi:10.1029/2002JD002347

Derr JS (1973) Earthquake lights: a review of observations and present theories. Bull Seis Soc Am 63:2177–2187

Derr JS (1986) Luminous phenomena and their relationship to rock fracture. Nature 321:470–471

Dobrovolsky IP, Zubkov SI, Miachkin VI (1979) Estimation of the size of earthquake preparation zones. Pure appl Geophys 117:1025–1044

Enomoto Y, Zheng Z (1998) Possible evidences of earthquake lightning accompanying the 1995 Kobe earthquake inferred from the Nojima fault gouge. Geophy Res Lett 25:2721–2724

Finkelstein D, Powell J (1970) Earthquake lightning. Nature 228:759–760

Freund F (2000) Time-resolved study of charge generation and propagation in igneous rocks. J Geophys Res 105:11001–11019

Harrison RG, Aplin KL, Rycroft MJ (2010) Atmospheric electricity coupling between earthquake regions and the ionosphere. J Atmos Sol Terr Phys 72:376–381

Harrison RG, Aplin KL, Rycroft MJ (2014) Brief communication: earthquake–cloud coupling through the global atmospheric electric circuit. Nat Hazards Earth Syst Sci 14:773–777

Hayakawa M (ed) (1999) Atmospheric and ionospheric electromagnetic phenomena associated with earthquakes. Terra Scientific Publishing Company, Tokyo, p 996

Hayakawa M, Fujinawa Y (eds) (1994) Electromagnetic phenomena related to earthquake prediction. Terra Scientific Publishing Company, Tokyo, p 677

Hayakawa M, Molchanov OA (eds) (2002) Seismo electromagnetics: lithosphere-atmosphere-ionosphere coupling. TERRAPUB, Tokyo, p 477
Heraud JA, Lira JA (2011) Co-seismic luminescence in Lima, 150 km from the epicenter of the Pisco, Peru earthquake of 15 August 2007. Nat Hazards Earth Syst Sci 11:1025–1036
Hosmer DW, Lemeshow S (1989) Applied logistic regression. Wiley, New York
Kim VP, Liu JY, Hegai VV (2012) Modeling the pre-earthquake electrostatic effect on the F region ionosphere. Adv Space Res 50:1524–1533
Kuo CL, Huba JD, Joyce G, Lee LC (2011) Ionosphere plasma bubbles and density variations induced by pre-earthquake rock currents and associated surface charges. J Geophys Res 116:A10317. doi:10.1029/2011JA016628
Kuo CL, Lee LC, Huba JD (2014) An improved coupling model for the lithosphere–atmosphere–ionosphere system. J Geophys Res 119:3189–3205. doi:10.1002/2013JA019392
Lay T, Wallace TC (1995) Modern global seismology. Elsevier, Amsterdam
Liu JY, Chen YI, Chuo YJ, Tsai HF (2001) Variations of ionospheric total electron content during the Chi-Chi earthquake. Geophys Res Lett 28:1383–1386
Liu JY, Chen YI, Chuo YJ, Chen CS (2006) A statistical investigation of preearthquake ionospheric anomaly. J Geophys Res 111:A05304. doi:10.1029/2005JA011333
Liu JY, Chen YI, Chen CH, Liu CY, Chen CY, Nishihashi M, Li JZ, Xia YQ, Oyama KI, Hattori K, Lin CH (2009) Seismo-ionospheric GPS total electron content anomalies observed before the 12 May 2008 Mw7.9 Wenchuan earthquake. J Geophys Res 114:A04320. doi:10.1029/2008JA013698
Liu JY, Chen YI, Chen CH, Hattori K (2010) Temporal and spatial precursors in the ionospheric global positioning system (GPS) total electron content observed before the 26 December 2004 M9.3 Sumatra–Andaman Earthquake. J Geophys Res 115:A09312. doi:10.1029/2010JA015313
Liu JY, Le H, Chen YI, Chen CH, Liu L, Wan W, Su YZ, Sun YY, Lin C, Chen MQ (2011) Observations and simulations of seismoionospheric GPS total electron content anomalies before the 12 January 2010 M7 Haiti earthquake. J Geophys Res 116:A04302. doi:10.1029/2010JA015704
Lockner DA, Johnston MJS, Byerlee JD (1983) A mechanism to explain the generation of earthquake lights. Nature 302:28–33
Pulinets S, Boyarchuk K (2004) Ionospheric precursors of earthquakes. Springer, New York
Pulinets S, Davidenko D (2014) Ionospheric precursors of earthquakes and global electric circuit. Adv Space Res 53:709–723
Rakov VA, Uman MA (2003) Lightning: physics and effects. Cambridge University Press, Cambridge
St-Laurent F, Derr JS, Freund FT (2006) Earthquake lights and the stress-activation of positive hole charge carriers in rocks. Phys Chem Earth 31:305–312